MOLECULAR AND CELLULAR BIOLOGY, Apr. 2004, p. 3514–3525 Vol. 24, No. 8
0270-7306/04/$08.00+0 DOI: 10.1128/MCB.24.8.3514–3525.2004

Muscle Regeneration and Myogenic Differentiation Defects in Mice Lacking TIS7

Santhosh K. Vadivelu,[1]† Robert Kurzbauer,[2] Benjamin Dieplinger,[1] Margit Zweyer,[3] Ralf Schafer,[3] Anton Wernig,[3] Ilja Vietor,[1]* and Lukas A. Huber[1]*

Institute for Anatomy, Histology, and Embryology, Department of Histology and Molecular Cell Biology, Medical University Innsbruck, A-6020 Innsbruck,[1] and Institute of Molecular Pathology, A-1030 Vienna,[2] Austria, and Department of Physiology and Neurophysiology, University of Bonn, D-53111 Bonn, Germany[3]

Received 12 September 2003/Returned for modification 14 November 2003/Accepted 14 January 2004

The tetradecanoyl phorbol acetate-induced sequence 7 gene (*tis7*) is regulated during cell fate processes and functions as a transcriptional coregulator. Here, we describe the generation and analysis of mice lacking the *tis7* gene. Surprisingly, TIS7 knockout mice show no gross histological abnormalities and are fertile. Disruption of the *tis7* gene by homologous recombination delayed muscle regeneration and altered the isometric contractile properties of skeletal muscles after muscle crush damage in TIS7$^{-/-}$ mice. Cultured primary myogenic satellite cells (MSCs) from TIS7$^{-/-}$ mice displayed marked reductions in differentiation potential and fusion index in a strictly cell-autonomous fashion. Loss of TIS7 caused the down-regulation of muscle-specific genes, such as those for MyoD, myogenin, and laminin-α2. Fusion potential in TIS7$^{-/-}$ MSCs could be rescued by TIS7 expression or laminin supplementation. Therefore, TIS7 is not essential for mouse development but plays a novel regulatory role during adult muscle regeneration.

Cell proliferation and differentiation are governed by different stimuli, including soluble growth factors, the extracellular matrix (1, 12), and direct cell-cell interactions (8). While each of these signals uniquely regulates mitogenic responses and gene activity, the proliferation, differentiation, or apoptosis of a cell is an integrated response to its adhesive and growth factor environments (18, 19).

The mouse *tis7* (*PC4*) gene was identified as an immediate-early gene specifically induced by tetradecanoyl phorbol acetate, epidermal growth factor, and fibroblast growth factor in Swiss 3T3 mouse cells and cultured rat astrocytes (2, 20). Vietor et al. showed previously that TIS7 is up-regulated after c-Jun activation in epithelial cells, translocates into the nucleus, and acts as a transcriptional coregulator (22). TIS7 can interact with mSin3B and histone deacetylase (HDAC) 1 as well as other members of the HDAC complex and is capable of specific transcriptional repression in an HDAC-dependent manner (22).

TIS7 was shown to be expressed in C2C12 myoblasts and in differentiated myotubes, with a transient decrease after the onset of differentiation (7). In vitro studies with C2C12 myoblasts and antisense *tis7* DNA transfection or microinjection of anti-TIS7 polyclonal antibodies caused a delay in myoblast differentiation (7). To define the essential functions of TIS7 in vivo, we have generated mice lacking a functional *tis7* gene by homologous recombination.

TIS7$^{-/-}$ mice are viable and fertile but develop an interesting muscle regeneration phenotype upon muscle crush damage (MCD). In addition, we identified several myoblast-specific genes involved in muscle regeneration as being regulated by TIS7. This phenotype can be recapitulated in vitro in TIS7$^{-/-}$ primary myogenic satellite cell (MSC) cultures and is characterized by an almost complete absence of fusion-competent MSCs. In addition, we identified several myoblast-specific genes involved in satellite cell function as being regulated by TIS7. These data demonstrate that TIS7 is not required for the normal development of the mouse embryo. In summary, we demonstrate a unique requirement for TIS7 in the differentiation of MSCs.

MATERIALS AND METHODS

Targeting of the murine *tis7* gene. Sequence information for the genomic locus of *tis7* was obtained by screening of a 129SV mouse genomic library in vector Lambda FIX II (Stratagene, La Jolla, Calif.) with a 5′-region probe of *tis7* cDNA. A 20.5-kb sequence contig covering exons 1 to 8 of *tis7* was generated by "primer walking." Herpes simplex virus thymidine kinase and diphtheria toxin α (DT-α) expression cassettes were cloned into plasmid pSP64. A 1.5-kb genomic fragment containing the first exon and part of exon 2 were generated by PCR with embryonic stem (ES) cell line E14.1 DNA as the template. A 5-kb genomic fragment containing exons 4 to 8 was isolated from a SalI subclone of the 129SV library. A *loxP*-flanked neomycin resistance cassette was inserted between the 1.5- and 5-kb homologous arms of the *tis7* genomic locus. A *lacZ* simian virus 40-pA cassette was cloned in frame to exon 2 (amino acid 43), which codes for a TIS7 (amino acids 1 to 43)- β-galactosidase fusion protein. ES cell line E14.1 was cultured on MTK-Neo feeder cells and electroporated (500 μF, 240 V) with the linearized targeting vector. ES cells were selected for ~9 days in the presence of neomycin (G418; 300 μg/ml), and colonies were screened for integration of the construct at the correct locus by PCR. One out of >1,000 screened colonies was also confirmed to be positive by Southern blot analysis. The targeted ES cells were injected into C57BL/6 blastocysts. Chimeric offspring were crossed with C57BL/6 mice to achieve heterozygous mice with germ line transmission. These heterozygous mice were subsequently bred to generate mice homozygous for the *tis7* deletion (TIS7$^{-/-}$).

MCD. All surgical procedures were carried out under halothane anesthesia and in strict accordance with National Health and Medical Research Council guidelines. In anesthetized mice, the soleus muscle was crushed from the pos-

* Corresponding author. Mailing address: Institute for Anatomy, Histology, and Embryology, Department of Histology and Molecular Cell Biology, Medical University Innsbruck, Mullerstr. 59, A-6020 Innsbruck, Austria. Phone: 43-512-507-3350. Fax: 43-512-507-2863. E-mail for Ilja Vietor: ilja.vietor@uibk.ac.at. E-mail for Lukas A. Huber: lukas.a.huber@uibk.ac.at.

† Present address: Cold Spring Harbor Laboratory, Cold Spring Harbor, NY 11724.

terior to the anterior tendons by exerting pressure with a pair of artery forceps for 10 s as described previously (4). The muscle was left in its bed with the tendons attached. After surgery, mice were transferred to standard cages with food and water ad libitum and allowed to recover in a temperature- and light-sensitive environment. Mice subjected to crush injury were sacrificed at different days after surgery as indicated in Results.

In vitro isometric tension measurements. Contraction measurements were performed 1 month after MCD as described previously (24). Soleus nerve-muscle preparations were dissected. Muscles were mounted in Lucite chambers perfused with aerated Tyrode solution (125 mM NaCl, 1.0 mM $MgCl_2$, 1.8 mM $CaCl_2$, 5.4 mM KCl, 24 mM $NaHCO_3$, 10 mM D-glucose) and connected to a force transducer. Muscle contractions were evoked either directly via a pair of silver electrodes in the bath or indirectly via nerve suction electrodes. Muscle length was adjusted so that maximal twitch tension was produced upon single stimuli. Voltage amplitudes were set to twice the lowest values sufficient for maximum twitch stimulation (final values were 20 to 25 V for direct muscle stimulation and 4 to 6 V for indirect muscle stimulation). Single pulses (0.5-ms duration for direct stimulation and 0.1-ms duration for indirect stimulation) and tetanic amplitudes of 20, 50, and 100 Hz for 2 s were used for stimulation.

The temperature was kept at 25.0 ± 0.5°C (mean and standard deviation) throughout the measurements. Muscles and nerves were stimulated alternately with single pulses and tetanic force in a sequence which was kept constant in all experiments. A minimum of 3 min was allowed for muscle recovery between stimulations. Signals were stored in a digital oscilloscope (model HM 208; Hameg, Frankfurt, Germany) and plotted on paper.

Acetylcholine (Ach) sensitivity was tested by rapid exchange of the normal perfusion solution with ACh-containing Tyrode solution (5 or 50 mg of ACh perchlorate $liter^{-1}$; Sigma). The amplitude of the evoked contracture was expressed as a fraction (percentage) of the amplitude of a preceding tetanus (100 Hz).

Isolation of primary myoblasts, cell cultures, and immunohistochemical analysis. Primary MSCs were isolated from lower hind limb muscle of 2- to 3-month-old adult mice as described previously (17a). The culture medium was supplemented with fibroblast growth factor 2 (2.5 ng/ml). Primary cell cultures were maintained on collagen-coated dishes (Roche) with growth medium (Ham's F-10 medium [E15-014; PAA Laboratories GmbH, Linz, Austria] supplemented with 20% fetal calf serum and penicillin-streptomycin [GIBCO BRL]). Purified laminin (Sigma) dissolved in phosphate-buffered saline (PBS) was used for coating Permanox slides (Nalge Nunc) for the rescue experiments. The medium was changed daily, and cultures were routinely passaged 1:3 as they reached 60 to 70% confluence. To maintain the characteristic features of the primary cell cultures, all experiments were performed with cultures that had passage numbers between 4 and 7. Differentiation medium consisted of DME medium (GIBCO BRL) supplemented with 5% horse serum and antibiotics as described above.

The purity of the MSC cultures and their differentiation potential were determined by c-met (SP260; Santa Cruz Biotechnology), desmin (Sigma), and myosin heavy-chain (MF20; Developmental Studies Hybridoma Bank) immunostaining. Briefly, myoblasts in growth medium were fixed with 4% paraformaldehyde in PBS and stained with anti-c-met antibodies and/or antidesmin antibodies. Major histocompatibility complex (MHC) expression was detected by fixing differentiated cultures with 90% methanol and staining with monoclonal antibody MF20. Immunostaining was performed as described previously ().

Northern, Western blot, and immunohistochemical analyses. To analyze *tis*7 gene expression, total RNA from various tissue samples was isolated and subjected to Northern analysis as described previously (22). The 555-bp probe was from the 5′ end of the cDNA and recognized specifically *tis7*. The myogenin, MyoD, and desmin probes were described previously (14). The probes for the laminin-α1 and laminin-α2 chains also were described previously (15). The amounts of loaded RNA were normalized by subsequent hybridization with the glyceraldehyde 3-phosphate dehydrogenase probe. To analyze TIS7 protein expression, total protein from various tissue samples was isolated and subjected to Western blot analysis as described previously (22). We used an affinity-purified rabbit polyclonal TIS7 antiserum raised against a peptide comprising 18 N-terminal amino acid residues of TIS7 as described previously (22). Western blot analysis with mouse antidesmin antibody (Chemicon International), rabbit anti-laminin-α1 antibody (Sigma), monoclonal anti-laminin-α2 antibody (Sigma), mouse anti-MyoD antibody 5A8 (PharMingen), mouse antimyogenin antibody F5D (Developmental Studies Hybridoma Bank), and antitubulin antibody (Sigma) was performed with extracts prepared from muscle tissue as described previously (14). Immunostaining was performed as described previously (21).

Differentiation time course measurements. To assay the differentiation potential of $TIS7^{+/+}$ and $TIS7^{-/-}$ MSCs, 10^3 low-passage cells in growth medium were seeded into each well of a four-well Permanox slide and cultured for an additional 24 h (day 0) before the addition of differentiation medium. On subsequent days (1 to 5), the cultures were fixed and immunostained for MHC with antibody MF20. To establish the differentiation potential of the cultures, at least 1,500 nuclei from MF20-positive cells were counted from several random fields. The percentage of differentiated cells was calculated as follows: (nuclei within MF20-stained myocytes/total number of nuclei) × 100. The fusion index was calculated as follows: (MF20-stained myocytes containing ≥2 nuclei/total number of nuclei) × 100. All experiments were performed in triplicate with three independent $TIS7^{+/+}$ and $TIS7^{-/-}$ MSC isolates.

Mixing of $TIS7^{-/-}$ and $TIS7^{+/+}$ MSC cultures. Early-passage $TIS7^{-/-}$ and $TIS7^{+/+}$ MSC cultures were labeled with a PKH26 red fluorescent cell linker kit (PKH26-GL; Sigma). PKH26-labeled and unlabeled primary cells were plated at an initial density of 10^3 cells per well in a four-well Permanox slide at ratios of $TIS7^{-/-}$ cells to $TIS7^{+/+}$ cells of 1:0, 1:4, 4:1, and 0:1. Duplicate cultures were grown overnight in growth medium before exposure to differentiation medium for 5 days. Wells were washed with PBS and fixed with 2% paraformaldehyde in PBS, and immunostaining was performed with antibody MF20 as described above.

Infection with Celo-TIS7 virus and generation of stable $TIS7^{-/-}$ MSC pools. Construction of a recombinant Celo virus expressing the TIS7 gene (Celo-TIS7 virus) was described previously (22). Construction of a recombinant Celo virus expressing green fluorescent protein (GFP) (Celo-GFP virus; Celo AIM53) was described previously (17). Low-passage subconfluent cultures of $TIS7^{-/-}$ MSCs were infected with either Celo-TIS7 or Celo-GFP virus as described previously (22). The cultures were refed 3 h after infection with growth medium and cultured for an additional 24 h before the addition of differentiation medium. The resulting colonies were pooled and expanded for further analysis. TIS7 expression was evaluated by Western blot analysis with anti-TIS7 or anti-Myc antibodies. GFP expression was evaluated by Western blot analysis with anti-GFP antibodies (Roche 1814460). The differentiation and fusion potentials of TIS7-expressing pools were assayed as described above.

RESULTS

Analysis of $TIS7^{-/-}$ mice. Genomic DNA fragments containing the mouse *tis7* gene isolated in our previous experiments were used for constructing a targeting vector (Fig. 1a). In order to inactivate the *tis7* gene, we generated a targeting construct interrupting exon 2 and deleting exon 3 of the *tis7* gene. A *lacZ* cassette was fused in frame to the first ATG initiation codon of exon 1, together with a neomycin selection cassette and flanking genomic sequences, as indicated in Fig. 1a. The targeted allele lacked part of exon 2 and exon 3. The rest of the *tis7* sequence (exons 4 to 8) was out of frame and therefore did not produce functional TIS7 protein. The ES clones harboring the targeted *tis7* gene were shown to have the expected arrangement of genomic DNA by Southern blot analysis with gene-specific probes (Fig. 1b). The *tis7* probe used for Northern blot analysis was 555 bp long and was from the 5′ end of the cDNA, which recognized specifically *tis7*. For Western blot analysis, we used an affinity-purified rabbit polyclonal TIS7 antiserum raised against a peptide comprising 18 N-terminal amino acid residues of TIS7 as described previously (22). Northern and Western blot analyses showed the absence of both TIS7 mRNA (Fig. 1c) and its protein product (Fig. 1d) in $TIS7^{-/-}$ mice, demonstrating that the introduced mutation was a null mutation of the gene. Interestingly, SKMc15, a homologue of TIS7, was not up-regulated in $TIS7^{-/-}$ mice (Fig. 1d). However, mice homozygous for the mutation, obtained by crossing heterozygous mice, were viable. $TIS7^{-/-}$ mice exhibited no obvious abnormality in reproduction under conventional housing conditions. Histological analyses of various tissues, including adult skeletal muscles, did not reveal any abnormalities in $TIS7^{-/-}$ mice at a younger age (3 to 6 months). However, at an older age (24 months), $TIS7^{-/-}$ mice

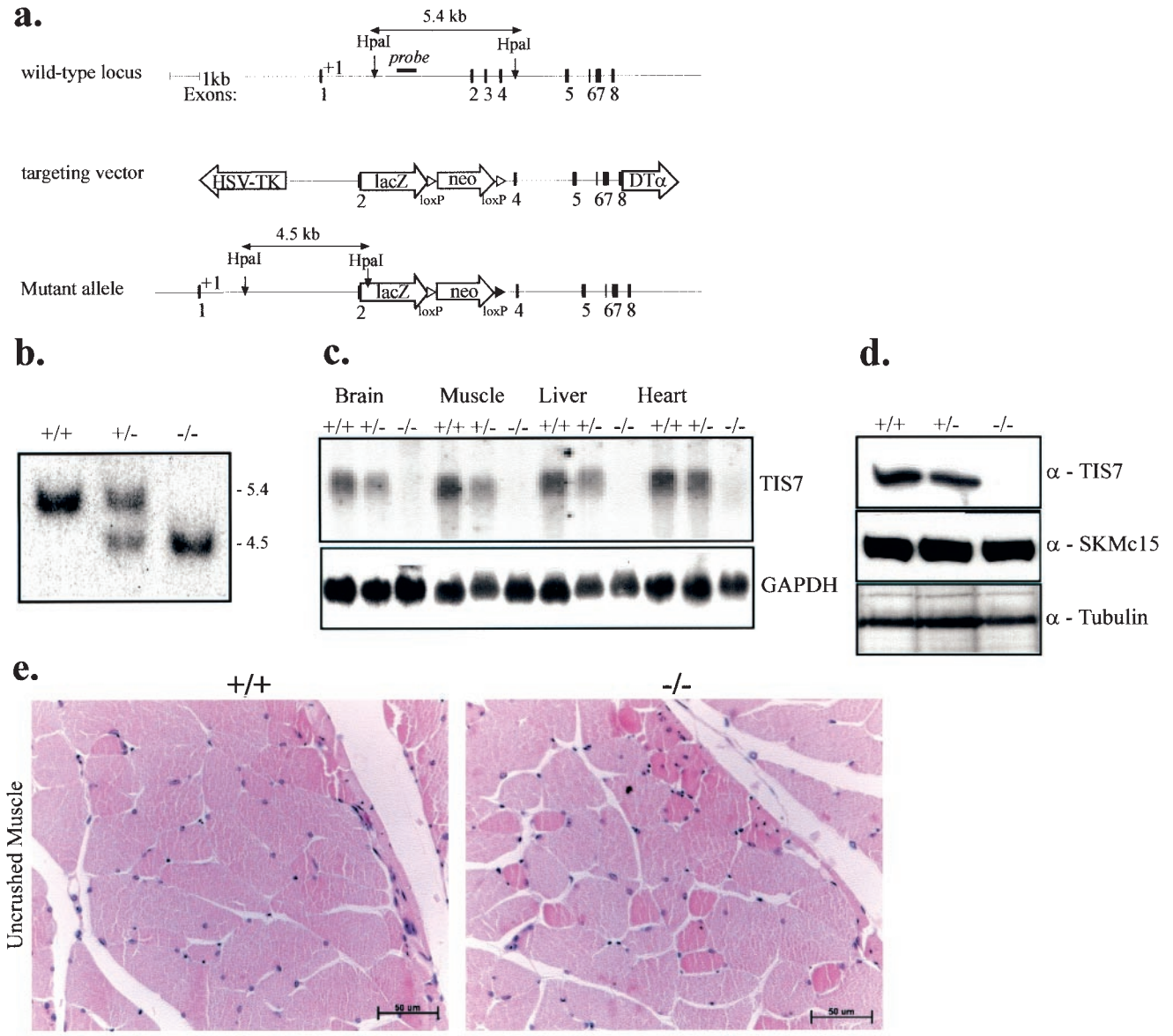

FIG. 1. Targeted disruption of the *tis7* gene and characterization of the null phenotype. (a) Homologous recombination with the targeting vector deletes part of exon 2 and exon 3, inserts the *lacZ* gene in frame with *tis7*, and brings exons 4 to 8 out of frame. Arrows indicate the orientations of the neomycin resistance (neo), *lacZ*, herpes simplex virus thymidine kinase, and DT-α cassettes. (b) Southern blot analysis demonstrates the genotypes of the offspring. A 5′-flanking probe (labeled "probe" in panel a) detects a 5.4-kb HpaI fragment in the wild-type allele and a 4.5-kb fragment in the targeted allele in mice. GAPDH, glyceraldehyde 3-phosphate dehydrogenase. (c) Northern blot analysis was performed with various tissues from the offspring. (d) Immunoblot analysis of TIS7 was performed with protein lysates from the soleus muscles of TIS7$^{+/+}$, TIS7$^{+/-}$, and TIS7$^{-/-}$ mice. (e) Hematoxylin-eosin-stained quadriceps muscle sections from TIS7$^{+/+}$ and TIS7$^{-/-}$ mice. Note the variations in fiber sizes in the knockout animals. Bars, 50 μm.

had a significantly lower whole-body weight than did TIS7$^{+/+}$ animals (mean and standard deviation, 39.44 ± 1.811 g [n = 11] versus 32.77 ± 1.294 g [n = 19]; P = 0.005). For this group of older TIS7$^{-/-}$ mice, we observed in several different skeletal muscles a statistically significant increase in the number of central nuclei, a smaller fiber diameter (Fig. 1e), a higher number of muscle fibers per field (smaller fibers), and a lower total number of fibers in the tibialis anterior muscle (Table 1 and Fig. 1e). We also observed a statistically significant decrease in the wet weight of the tibialis anterior muscle for TIS7$^{-/-}$ mice (0.08014 ± 0.004 g versus 0.05435 ± 0.003 g [n = 8]; P = 0.0001). Therefore, we examined the requirement for TIS7 in the maintenance and regeneration of adult muscle tissue after MCD in younger (4-month-old) mice.

Since TIS7 is expressed in embryonic skeletal muscles (3) and at high levels in adult skeletal muscles (Fig. 2a), we expected to find defects during adult muscle regeneration. First, we examined whether TIS7 is regulated during adult muscle regeneration in TIS7$^{+/+}$ mice after MCD of the soleus muscle. Initially, the spatial distribution of TIS7 in the adult TIS7$^{+/+}$

TABLE 1. Muscle analyses[a]

Mice	Muscle	Mean ± SEM (no. of experiments)			
		% of central nuclei in muscle fibers	Muscle fiber diam (μm)	No. of muscle fibers	
				Per field	Total
TIS7$^{+/+}$	Quadriceps	3.408 ± 0.09124 (3)	59.01 ± 0.5641 (1,595)	54.45 ± 4.509 (29)	
	Tibialis anterior	4.364[b] (1)	39.15 ± 0.4609 (550)	113.4 ± 6.071 (5)	1,404 (1)
	Gastrocnemius	2.825[b] (1)	44.32 ± 0.6001 (531)		
TIS7$^{-/-}$	Quadriceps	7.226 ± 0.2795 (3)[c]	43.76 ± 0.3652 (1,603)[d]	72.95 ± 6.588 (22)[e]	
	Tibialis anterior	7.045[b] (1)	33.28 ± 0.4447 (582)[d]	150.8 ± 11.86 (4)[e]	1,154 (1)
	Gastrocnemius	8.560[b] (1)	40.05 ± 0.5344 (513)[d]		

[a] The indicated muscles were dissected from 24-month-old male TIS7$^{+/+}$ and TIS7$^{-/-}$ mice, and samples were embedded in paraffin. Transverse 6-μm sections were cut through the middle of the muscle and stained with hematoxylin and eosin. The sections were photographed with a Zeiss Axioplan microscope, and measurement analysis was performed with Axiovision 4.1 software. The data were compared by using an unpaired Student *t* test. *P* values are for comparisons of data for TIS7$^{-/-}$ mice to data for TIS7$^{+/+}$ mice. Muscle fiber diameter was measured as the longest diameter of each muscle fiber. For each experiment, at least 500 fibers were used.
[b] Mean only.
[c] *P* value, 0.0002.
[d] *P* value, <0.0001.
[e] *P* value, <0.05.

soleus muscle was analyzed by immunofluorescence. Interestingly, TIS7 showed specific immunoreactivity around the myofibers (Fig. 2a).

TIS7 protein expression during the course of muscle regeneration in TIS7$^{+/+}$ mice was analyzed by immunofluorescence (Fig. 2b, c, and d) and Western blot analysis (Fig. 2f). Immunofluorescence analysis revealed TIS7 localization in the central myonuclei of the regenerating muscle fibers (Fig. 2b), consistent with its putative role as a transcriptional coregulator in muscle regeneration (22). The transient increases in TIS7 protein expression and nuclear localization were observed only during the regenerative stages and returned to basal levels by 30 days postoperation (Fig. 2f). Interestingly, we observed that SKMc15 protein expression was not regulated during the regenerative stages (Fig. 2f). This observation suggested a specific role for TIS7 during adult muscle regeneration in vivo.

Muscle regeneration after MCD is impaired in TIS7$^{-/-}$ mice. Given the marked up-regulation of TIS7 protein in regenerating muscles and its localization in the centrally located myonuclei in regenerating myofibers, it was of interest to search for deficits in muscle regeneration in TIS7$^{-/-}$ animals before and after MCD. This was done by functional assessment of soleus muscle contractile performance before and after MCD, respectively (Tables 2 and 3). The force was analyzed with isolated soleus muscle from age- and sex-matched TIS7$^{+/+}$ and TIS7$^{-/-}$ mice.

Interestingly, before MCD, a small (~10%) difference in body weight and a similar difference in the wet weight of the soleus muscle were detectable (Table 2). Maximum contractile tensions produced by isolated soleus muscle were similar in the TIS$^{-/-}$ and TIS7$^{+/+}$ animals, while specific tensions, i.e., force produced per unit of muscle mass, were lower in TIS7$^{-/-}$ animals than in TIS7$^{+/+}$ animals. Importantly, no deficits in muscle innervation were detectable, since sensitivities to bath-applied ACh, a stringent indicator for the amount of extrasynaptic receptors for ACh, were similar in TIS7$^{+/+}$ and TIS7$^{-/-}$ animals (Table 2). From our initial assessment of contractile functions of undamaged soleus muscle, we observed a weak and smaller soleus muscle in TIS7$^{-/-}$ mice, consistent with the lower body weight of the TIS7$^{-/-}$ mice. However, the undamaged soleus muscle from TIS7$^{-/-}$ mice was functionally similar to that from TIS7$^{+/+}$ mice (Table 2).

Measurements of force for isolated soleus muscle differed markedly between TIS7$^{+/+}$ and TIS7$^{-/-}$ mice after MCD (Table 3). After 30 days of regeneration, the single twitch and tetanus force of the TIS7$^{-/-}$ soleus muscle was significantly lower than that of the TIS7$^{+/+}$ soleus muscle (Table 3). Only after 5 to 7 weeks was the soleus muscle from TIS7$^{-/-}$ mice able to respond to the stimulation and generate a significant force similar to that of the soleus muscle from TIS7$^{+/+}$ mice (data not shown). Thus, a clear retardation in the recovery of contractile force development was present, and recovery was still incomplete by 5 weeks. Upon direct electrical stimulation, the TIS7$^{-/-}$ muscle developed a tetanic force approximately 60% that of the TIS7$^{+/+}$ muscle (Table 3). In addition, force production per unit of muscle weight (specific force; Table 3) remained significantly lower in regenerating TIS7$^{-/-}$ muscle, mainly due to a relatively high wet muscle weight, again indicating retarded muscle regeneration. In parallel, the reinnervation process seemed to be delayed; by 4 weeks, reinnervation was complete in TIS7$^{+/+}$ animals (degree of innervation, 97 to 98%) and amounted to 73 and 87% for twitch stimulation and tetanic stimulation, respectively, in TIS7$^{-/-}$ animals. Faithfully accompanying such deficits in nerve-evoked stimulation, muscle ACh sensitivity was significantly increased in TIS7$^{-/-}$ animals. After 4 to 5 weeks, ACh sensitivity in TIS7$^{+/+}$ mice had returned to normal values, while it was still higher in TIS7$^{-/-}$ mice. After the contractile tension measurements were recorded, all muscles were frozen, and the amount of crush-induced damage was assessed as the frequency of centrally located myonuclei in the regenerated myofibers (data not shown).

Analysis of muscle-specific gene expression in TIS7$^{-/-}$ muscle tissue. To gain further insight into the regeneration defect in TIS7$^{-/-}$ mice, total RNA and protein samples from uncrushed soleus muscles were prepared from TIS7$^{+/+}$, TIS7$^{+/-}$, and TIS7$^{-/-}$ mice ($n = 3$). Western and Northern blot analyses were performed with a panel of muscle-specific antibodies and cDNA probes. The expression of muscle regulatory factors was investigated to elucidate the regulatory relationships and

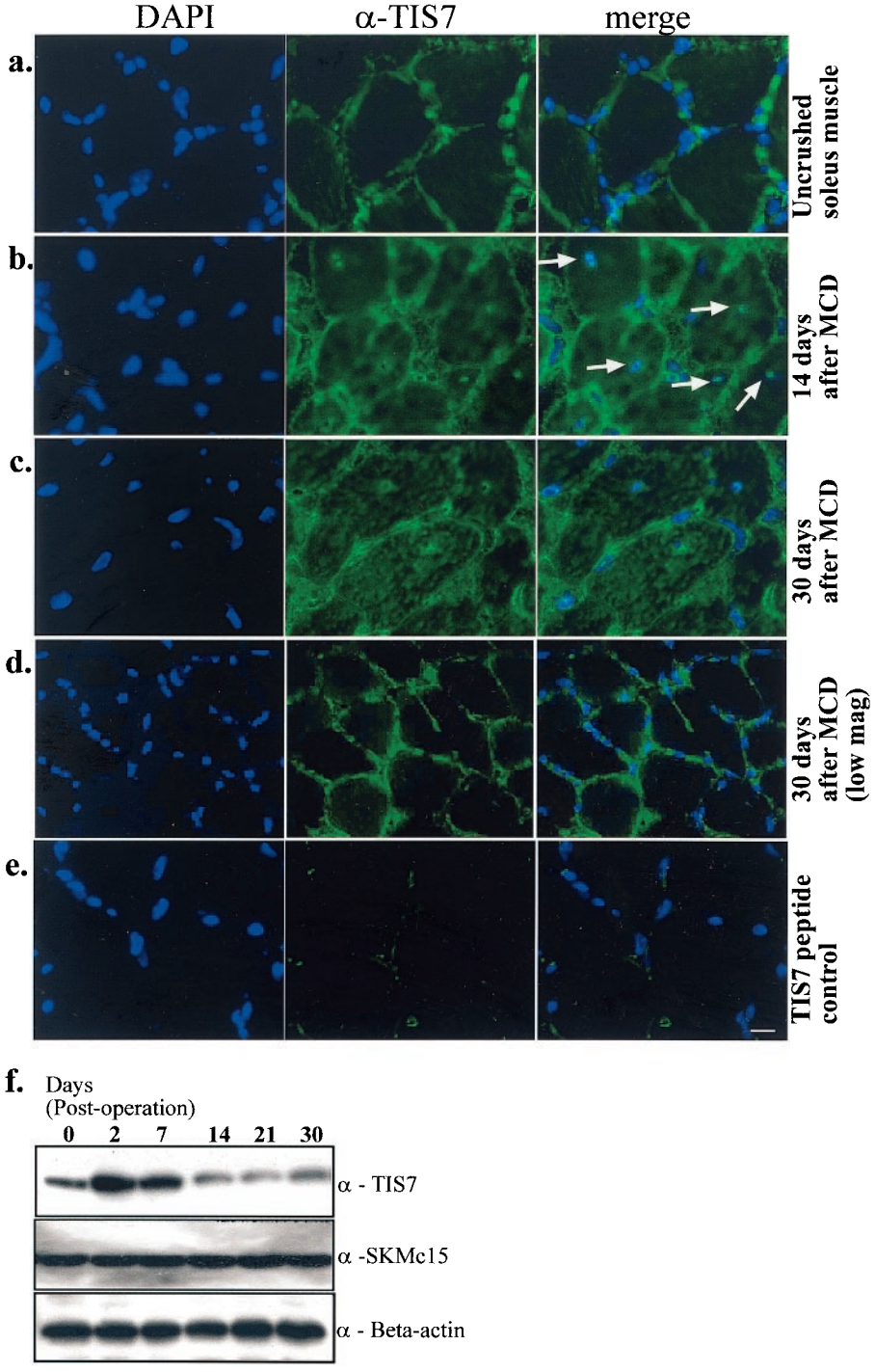

FIG. 2. (a) Typical TIS7 localization in uncrushed soleus muscle. For immunofluorescence analysis of soleus muscle from TIS7$^{+/+}$ mice, fixed cryosections were stained with TIS7 polyclonal antibody. DAPI, 4′,6′-diamidino-2-phenylindole. (b) Fourteen days after MCD. (c and d) Thirty days after MCD. Note the increased expression and nuclear localization of TIS7 after the crush injury, with a typical central location of nuclei (arrows in panel b). These findings were transitory in the initial phase of regeneration. Increased TIS7 expression and central location of nuclei were also detectable in a few regenerating fibers after 30 days (high-magnification image [c]). In general, the localization was similar to that observed in control sections (uncrushed soleus muscle) (low-magnification [mag] image, 30 days [d]). (e) TIS7 peptide inhibition showing TIS7 antibody specificity in the soleus muscle. Bar, 50 μm. (f) Western blot analysis of lysates prepared from uncrushed or crushed soleus muscle. Blots were probed with TIS7 and SKMc15 polyclonal antibodies. Equal protein loading was confirmed by probing with α-beta-actin antibody. Note that upon MCD, TIS7 protein expression was up-regulated and peaked by 12 h; this transient increase was reduced after 30 days.

TABLE 2. Isometric contractile properties of soleus muscles before MCD[a]

Parameter	Mean ± SD for the following mice:	
	TIS7$^{-/-}$	TIS7$^{+/+}$
Whole body wt (g)	33.4 ± 0.6[b]	36.2 ± 2.0
Wet muscle wt (mg)	17.3 ± 2.2	19.7 ± 2.0
Maximum tetanic force direct stimulation (mN)	196.6 ± 8.8	210 ± 10.4
Maximum twitch force direct stimulation (mN)	31.1 ± 1.4[b]	34.8 ± 1.1
Specific force (N/g)	11.1 ± 0.6[b]	13.2 ± 0.4
% Contracture with ACh (50 mg/liter)	1.2 ± 0.8	1.7 ± 1.2

[a] Soleus muscles from 4-month-old mice were studied before MCD.
[b] Statistical analysis (unpaired Student *t* test) revealed a *P* value of <0.05 in a comparison of TIS7$^{+/+}$ (n = 4) and TIS7$^{-/-}$ (n = 4) animals.

the potential for functional compensation in the absence of TIS7. Western and Northern blot analyses showed that MyoD, which was expressed at high levels in TIS7$^{+/+}$ soleus muscle, was expressed at significantly lower levels in TIS7$^{-/-}$ soleus muscle (Fig. 3a and b). In addition, the relative levels of myogenin mRNA and protein in TIS7$^{-/-}$ soleus muscle remained significantly lower than those in TIS7$^{+/+}$ soleus muscle (Fig. 3a and b), whereas desmin mRNA levels were down-regulated in TIS7$^{-/-}$ soleus muscle (Fig. 3b). Western blot analysis of desmin in lysates of TIS7$^{-/-}$ and TIS7$^{+/+}$ muscles showed no obvious difference in protein levels (Fig. 3a).

A deficiency of laminin-α2 is known to cause muscular dystrophies in humans and animals. Surprisingly, we detected low levels of laminin-α2 in TIS7$^{-/-}$ soleus muscle (Fig. 3a and b) at both the mRNA and the protein levels. We also confirmed the low levels of laminin-α2 in TIS7$^{-/-}$ soleus muscle by immunofluorescence analysis (Fig. 3c). Interestingly, there was no significant change in the laminin-α1 mRNA and protein

TABLE 3. Isometric contractile properties of regenerated soleus muscles[a]

Parameter	Mean ± SD for the following mice:	
	TIS7$^{-/-}$	TIS7$^{+/+}$
Whole body wt (g)	26.0 ± 2.8[b]	32.1 ± 3.2
Wet muscle wt (mg)	11.5 ± 1.2[b]	13.0 ± 1.0
Maximum tetanic force direct stimulation (mN)	87.7 ± 6.8[b]	136.2 ± 6.3
Maximum twitch force direct stimulation (mN)	19.3 ± 2.0[b]	28.6 ± 2.0
Specific force (N/g)	8.1 ± 0.7[b]	12.2 ± 0.5
% Twitch/tetanus ratio	17.6 ± 0.7[b]	20.8 ± 1.2
Maximum tetanic force indirect stimulation (mN)	105.0 ± 10.0[b]	159.6 ± 11.7
Maximum twitch force indirect stimulation (mN)	15.0 ± 1.6[b]	30.3 ± 1.7
% Degree of innervation with tetanic stimulation	87.9 ± 1.1[b]	97.2 ± 2.7
% Degree of innervation with twitch stimulation	72.0 ± 1.8[b]	98.8 ± 1.5
% Contracture with ACh (50 mg/liter)	16.1 ± 1.7[b]	3.1 ± 1.5

[a] Soleus muscles from 3- to 10-month-old mice were studied after MCD. For brevity, overall means for different age groups are shown here.
[b] Statistical analysis (unpaired Student *t* test) revealed a *P* value of <0.001 in a comparison of TIS7$^{+/+}$ (n = 18) and TIS7$^{-/-}$ (n = 18) animals.

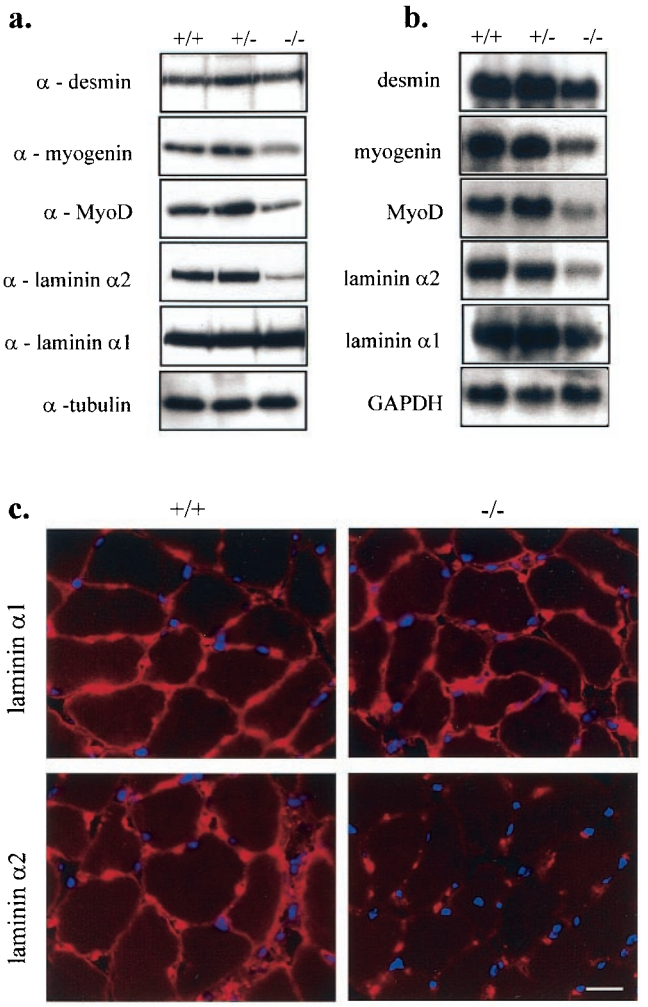

FIG. 3. (a) Western blot analysis of muscle protein lysates prepared from TIS7$^{+/+}$, TIS7$^{+/-}$, and TIS7$^{-/-}$ mice with muscle-specific markers. (b) Northern blot analysis of total mRNA prepared from TIS7$^{+/+}$, TIS7$^{+/-}$, and TIS7$^{-/-}$ mice with muscle-specific markers. GAPDH, glyceraldehyde 3-phosphate dehydrogenase. (c) Immunofluorescence analysis of soleus muscle for laminin expression in TIS7$^{+/+}$ and TIS7$^{-/-}$ mice. Fixed cryosections were stained with respective laminin antibodies. Note the reduced expression of laminin-α2 but the lack of effect on laminin-α1 in the soleus muscle from TIS7$^{-/-}$ mice. Bar, 50 μm.

levels in TIS7$^{-/-}$ soleus muscle compared to TIS7$^{+/+}$ soleus muscle (Fig. 3a and b). Consistently, we did not observe increased expression of laminin-α1 in TIS7$^{-/-}$ muscle by immunofluorescence analysis (Fig. 3c). Taken together, these results provide evidence that the expression of myogenic regulatory factors which affect muscle regeneration after MCD is changed in TIS7$^{-/-}$ mice.

TIS7$^{-/-}$ myogenic cultures have reduced differentiation potential. The results of the electrophysiology experiments indicating a delay in regeneration and the misregulation of important muscle regulatory proteins in TIS7$^{-/-}$ adult muscles suggested that TIS7 may play an important role in the differentiation of MSCs. To evaluate the differentiation potential of the TIS7$^{-/-}$ MSC cultures, the extent of myogenic differentiation was assessed at the cellular level by immunostaining

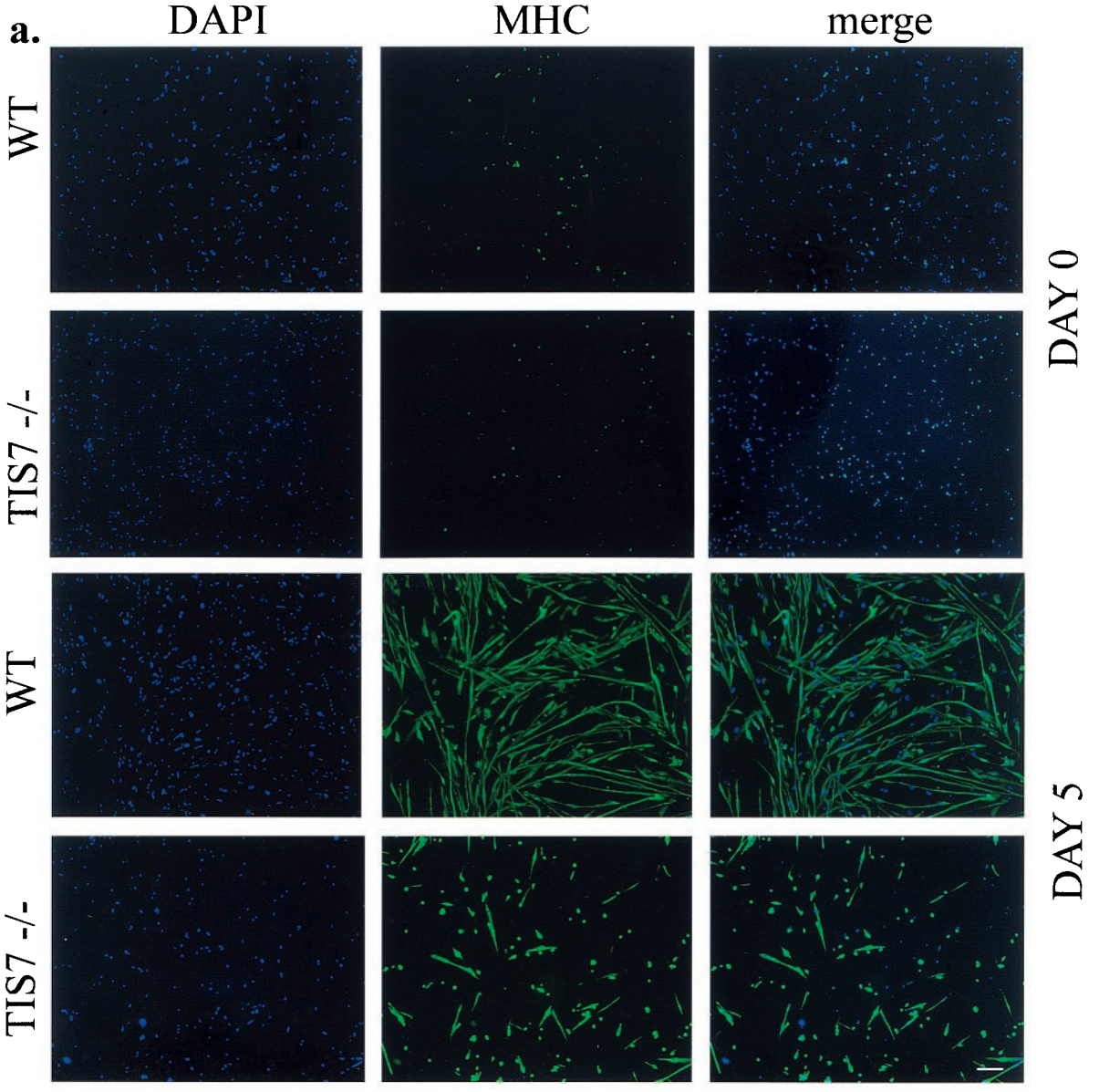
a.
DAPI
MHC
merge
WT
TIS7 -/-
WT
TIS7 -/-
DAY 0
DAY 5

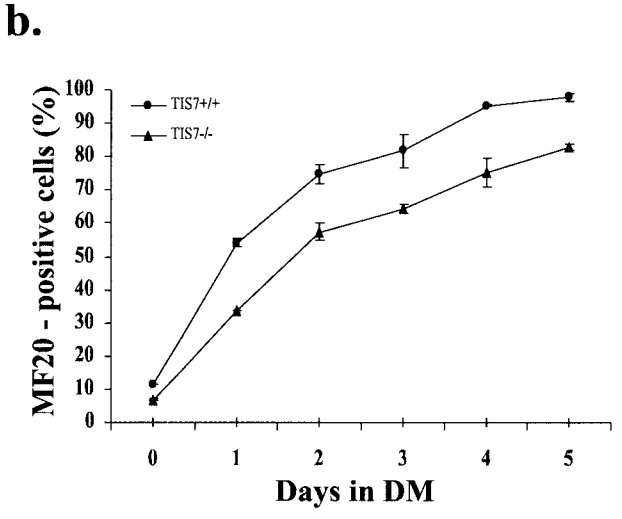
b.
MF20 - positive cells (%)
TIS7+/+
TIS7-/-
Days in DM

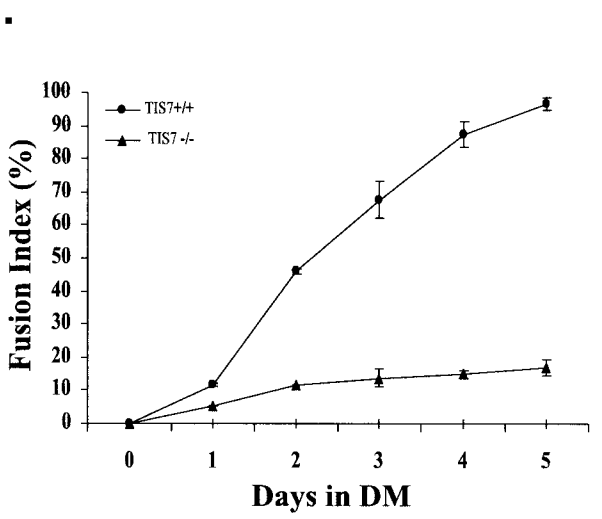
c.
Fusion Index (%)
TIS7+/+
TIS7 -/-
Days in DM

cultures fixed at daily intervals after mitogen withdrawal with antibody MF20, specifically recognizing MHC (Fig. 4a). Importantly, this analysis was performed with four independently isolated TIS7$^{+/+}$ and TIS7$^{-/-}$ primary MSC cultures. The establishment and propagation of stable cell lines can potentially result in aneuploidy as well as the introduction of additional mutations necessary for immortalization and continuous proliferation in cultures. To avoid such anomalies, all of our analyses were carried out with newly established low-passage primary MSC cultures. The purity of the MSC cultures was always 90 to 95%, as determined by antidesmin staining (data not shown).

The proportion of MHC-positive cells and the fusion index for both TIS7$^{+/+}$ and TIS7$^{-/-}$ cultures were assessed (Fig. 4b and c). To establish the differentiation potential of the cultures, at least 1,500 nuclei from MHC-positive cells were counted from several random fields. The percentage of differentiated cells was calculated as follows: (number of nuclei within MHC-stained myocytes/total number of nuclei) $\times$ 100. TIS7$^{-/-}$ MSCs expressed normal levels of hepatocyte growth factor receptor c-met, desmin, and vimentin but reduced levels of MyoD and myogenin compared to TIS7$^{+/+}$ MSCs (data not shown). Under growth conditions, TIS7$^{-/-}$ MSCs exhibited a reduction in the rate of spontaneous differentiation (mean and standard deviation, 4.0% $\pm$ 0.8%) compared to TIS7$^{+/+}$ MSCs (10.6% $\pm$ 1.5%) (day 0 in Fig. 4b). Consistent with this observation, TIS7$^{-/-}$ MSC cultures displayed a severe defect in the ability to differentiate and form multinucleated myotubes after mitogen withdrawal (Fig. 4a). After 24 h in differentiation medium, about 50% of the cells in TIS7$^{+/+}$ cultures began to undergo terminal differentiation. The number of differentiated TIS7$^{+/+}$ myotubes continued to accumulate in a linear manner, reaching ~94% at 5 days after mitogen withdrawal (Fig. 4b). Calculation of the fusion index revealed a marked reduction in the fusion capacity of TIS7$^{-/-}$ cultures (Fig. 4c). The fusion index was calculated as follows: (number of MHC-stained myocytes containing $\geq$2 nuclei/total number of nuclei) $\times$ 100. The fusion index of differentiated TIS7$^{+/+}$ cultures was ~95% after 5 days of differentiation, with a mean and standard deviation of 5.1 $\pm$ 0.4 nuclei per myotube (n = 500). In contrast, by day 5, only about 14% of TIS7$^{-/-}$ myocytes contained $\geq$2 nuclei, with an average of 1.1 $\pm$ 0.4 nuclei per myotube (n = 500) (Fig. 4c).

The TIS7$^{-/-}$ cellular phenotype is a cell-autonomous deficit. The reduced fusion potential and the continued proliferation of TIS7$^{-/-}$ MSCs under conditions that normally promote cell cycle withdrawal and terminal differentiation could be cell autonomous. For example, the marked reduction in the expression of MyoD and laminin-α2 (Fig. 3a and b) in TIS7$^{-/-}$ myogenic cells could inhibit differentiation. Alternatively, TIS7$^{-/-}$ MSCs may have a unique developmental identity that precludes participation in the myogenic precursor cell differentiation program. To explore these possibilities, we mixed different ratios of TIS7$^{+/+}$ and TIS7$^{-/-}$ MSCs. Subsequently, differentiation was induced by culturing the cells in differentiation medium for 5 days (Fig. 5a to d). PKH26 red fluorescent labeling was used for tracing of TIS7$^{-/-}$ MSCs in the cocultures. Importantly, PKH26 red fluorescent labeling did not affect terminal differentiation, as shown by labeling of TIS7$^{+/+}$ MSCs (Fig. 5d). As expected, the fusion potential of PKH26-labeled TIS7$^{-/-}$ MSCs was significantly lower when they were mixed with unlabeled TIS7$^{-/-}$ MSCs (Fig. 5a). To test whether TIS7$^{-/-}$ MSCs were affected by the presence of TIS7$^{+/+}$ MSCs, we mixed PKH26-labeled TIS7$^{-/-}$ MSCs with unlabeled TIS7$^{+/+}$ MSCs at ratios of 4:1 (Fig. 5b) and 1:4 (Fig. 5c). Strikingly, PKH26-labeled TIS7$^{-/-}$ MSCs were rarely detected within myotubes containing more than two nuclei (Fig. 5b and c). Conversely, the fusion potential of TIS7$^{+/+}$ MSCs was unaffected by the presence of high numbers of TIS7$^{-/-}$ MSCs, as shown in Fig. 5e. These data support the notion that TIS7 expression may define a distinct cell identity in the muscle satellite cell developmental program.

Rescue of the TIS7$^{-/-}$ cellular phenotype. Our analyses suggested that in the muscle satellite cell-derived myogenic cell lineage, important aspects of cytomorphology, differentiation, and ultimately fusion of mononuclear cells into myotubes were dependent on TIS7 activity. To determine whether the observed phenotypic differences between TIS7$^{-/-}$ and TIS7$^{+/+}$ MSCs were attributable to the presence of TIS7, a Celo-TIS7 recombinant adenovirus (22) was used to infect low-passage TIS7$^{-/-}$ MSCs (TIS7-CT), and pools of transfectants were analyzed (Fig. 6c and f). Western blot analysis indicated that infected TIS7-CT MSCs expressed the exogenous TIS7 protein (Fig. 6j). As expected, TIS7$^{-/-}$ MSCs which either were not infected or were infected with the Celo-GFP isotypic adenovirus control (TIS-CG) did not express the TIS7 protein (Fig. 6j). In growth medium, pools of TIS7-CT cells displayed an almost complete reversion of the fibroblast-like phenotype and exhibited a rounded compact cytomorphology similar to that of TIS7$^{+/+}$ MSCs. Transfer of TIS7-CT cultures into differentiation medium resulted in increased numbers of MHC-positive differentiated myotubes that displayed an elongated bipolar multinucleated morphology typical of TIS7$^{+/+}$ myotubes (Fig. 6c). After 3 days in differentiation medium, the TIS7-CT pools displayed fusion indices comparable to those of TIS7$^{+/+}$ cultures and approximately fivefold higher than those of TIS7$^{-/-}$ cultures (Fig. 6i, compare bars c and b). Differentiated TIS7-CT myotubes contained 2.6 $\pm$ 0.3 (mean and standard

FIG. 4. Reduced differentiation potential of TIS7$^{-/-}$ MSCs. (a) Differentiated myocytes were detected by immunostaining with antibody MF20, which is reactive with MHC. Incubation of TIS7$^{+/+}$ MSC cultures in differentiation medium resulted in a rapid increase in MHC synthesis and the formation of elongated multinucleated myotubes. In contrast, TIS7$^{-/-}$ MSCs differentiated with reduced kinetics and failed to form multinucleated elongated myotubes. Note the reduction in the rate of spontaneous differentiation observed for TIS7$^{-/-}$ cultures under growth conditions (day 0). Day 5 corresponds to the time in differentiation medium before staining, whereas day 0 represents cultures in growth medium. Bar, 20 μm. 4′,6′-Diamidino-2-phenylindole (DAPI) staining is shown as a control for equal cell density in the MSC differentiation assays. WT, wild type. (b) The percentage of MF20-positive cells was determined by enumeration of MHC-expressing differentiated myotubes by immunostaining with antibody MF20. DM, differentiation medium. (c) Calculation of fusion indices as percentages of cells containing two or more nuclei within a differentiated myotube confirmed that TIS7$^{-/-}$ MSCs were severely deficient in fusion capacity.

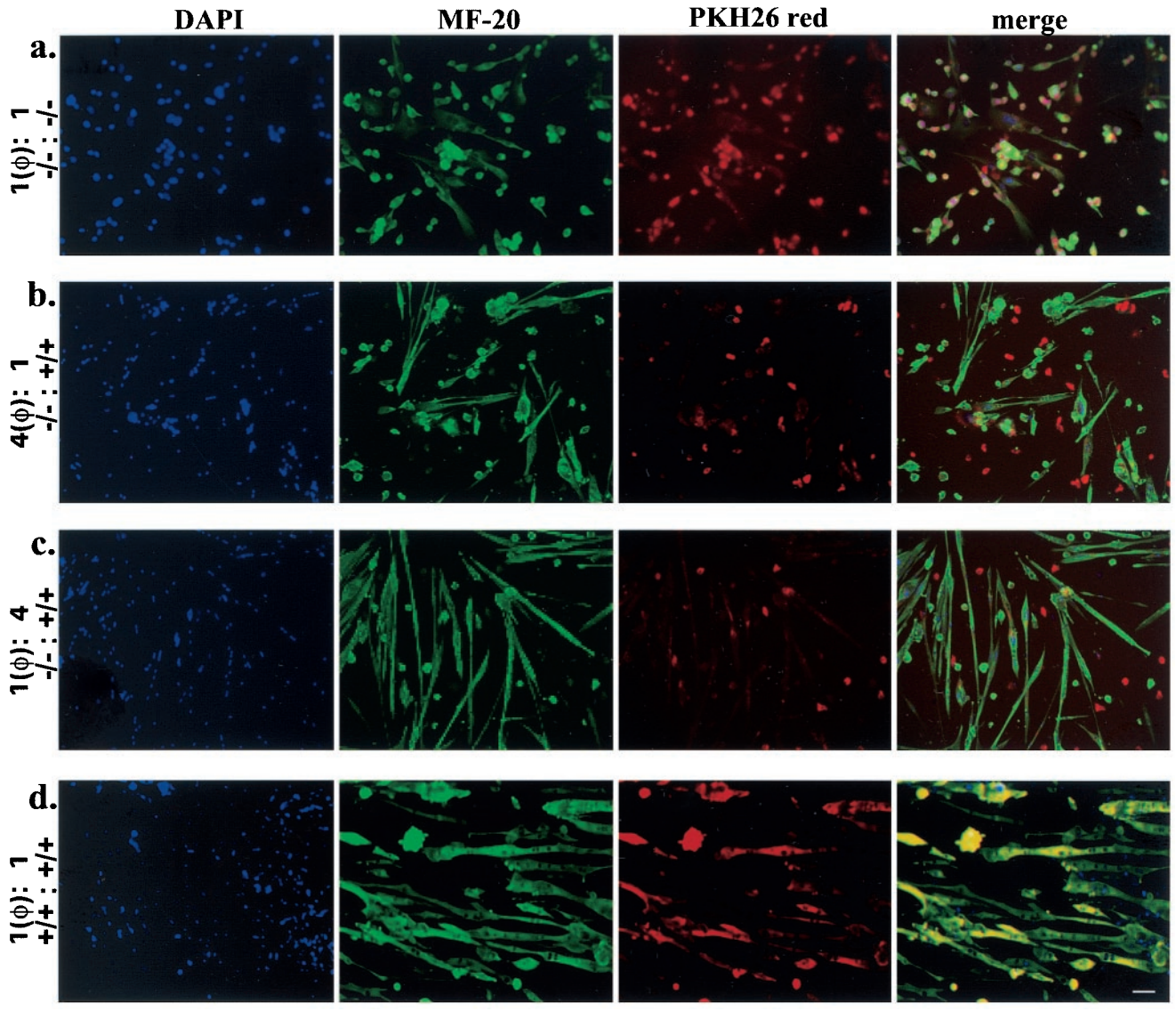

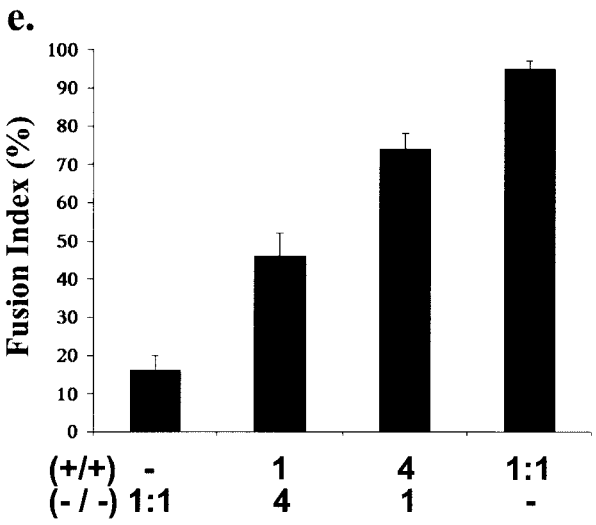

FIG. 5. Strict cell autonomy in differentiated cocultures of TIS7$^{-/-}$ and TIS7$^{+/+}$ MSCs. PKH26 red fluorescent labeling (ϕ) was used for cell tracing in the cocultures. (a) Primary MSCs were plated at the following ratios: labeled TIS7$^{-/-}$ to unlabeled TIS7$^{-/-}$ cells (1ϕ:4) (a), labeled

deviation) nuclei/myotube ($n = 500$). Differentiated TIS7$^{+/+}$ myotubes contained 2.8 ± 0.1 nuclei/myotube ($n = 500$). However, differentiated TIS7$^{-/-}$ myotubes contained only 1.1 ± 0.4 nuclei/myotube ($n = 500$) (Fig. 6b). Interestingly, culturing of TIS7$^{-/-}$ MSCs on slides coated with purified laminins rescued the differentiation potential but not the cytomorphology of the myotubes (Fig. 6e). This cytomorphological defect of TIS7$^{-/-}$ MSCs could be partially rescued by infection with the recombinant Celo-TIS7 adenovirus and culturing of TIS7-CT MSCs on slides coated with purified laminins (Fig. 6f). These observations showed that the expression of TIS7 was necessary and sufficient to reestablish the progression of TIS7$^{-/-}$ MSCs through the myogenic differentiation program.

DISCUSSION

TIS7 is required for MSC differentiation and fusion. Our results suggested that TIS7$^{-/-}$ adult muscle regeneration was defective in two aspects of regeneration: (i) deregulation of myogenic regulatory proteins and (ii) impaired differentiation and fusion potential of MSCs. MSC cultures isolated from TIS7$^{-/-}$ mice were unable to fuse and had a reduced differentiation potential. It was also evident from the cell tracing experiments that TIS7$^{-/-}$ MSCs had no influence on the differentiation of TIS7$^{+/+}$ MSCs and that TIS7$^{-/-}$ MSCs did not fuse with differentiating TIS7$^{+/+}$ myotubes. Taken together, these data support the notion that the loss of fusion potential is a consequence of a cell-autonomous defect in TIS7$^{-/-}$ MSCs. Moreover, TIS7 expression may define a distinct cell identity in the MSC developmental program. Forced expression of a functional TIS7 protein in TIS7$^{-/-}$ MSCs was sufficient to reverse the TIS7$^{-/-}$ cytomorphology and rescue the differentiation defect, as evidenced by a significant increase in the fusion index of TIS7-CT cells (Fig. 6i).

Myogenic precursor cells withdraw irreversibly from the cell cycle as they differentiate into mature myotubes. Cell cycle exit occurs early during the differentiation program and is required for normal expression of the contractile phenotype (23). TIS7$^{-/-}$ MSCs displayed inefficient withdrawal from the cell cycle in response to low levels of mitogen. Thus, we can conclude that TIS7 is not essential for MSC proliferation under growth conditions that normally induce cell cycle withdrawal and terminal differentiation. Therefore, characterization of cell cycle control in TIS7$^{-/-}$ MSCs should elucidate the role of TIS7 in cell cycle withdrawal and MSC differentiation.

Our data suggest that TIS7 is required for MSCs to become fusion-competent myogenic precursor cells expressing myogenic markers such as MyoD, laminin-α2, and myogenin. Consistent with the observed decreases in myogenin mRNA and protein levels, TIS7$^{-/-}$ MSCs displayed a reduction in the rate of spontaneous differentiation. It has been shown that MyoD plays an essential role in regulating the MSC myogenic program and that muscle regeneration is severely deficient in MyoD$^{-/-}$ mice (16). Moreover, the absence of MyoD in regenerating skeletal muscle affects the patterns of expression of the basement membrane, the interstitial matrix, and integrin molecules, consistent with delayed myotube formation (10). Clearly, further analysis of the developmental potential and phenotype of primary TIS7$^{-/-}$ MSCs may present a unique opportunity to investigate the early myogenic program of satellite cells.

The regeneration defect provoked by reduced levels of laminin-α2 in TIS7$^{-/-}$ mice is reminiscent of mice lacking a specific laminin isoform (25). In *Drosophila*, mutation of the only known laminin-α chain is embryonic lethal, leading to defects in numerous tissues (5, 9, 26). Defects in the central nervous system and in the development of the eye have been reported to be associated with laminin-α2-deficient human congenital muscular dystrophies, in particular, the Fukuyama-type and Walker-Warburg syndromes (6). However, these defects are not as severe as those observed in skeletal muscle, possibly due to the expression of other laminin isoforms at these sites compensating for the loss of laminin-α2. It appears that compensating and/or stabilizing factors such as growth factors and extracellular matrix from nonmuscle cells may be present in vivo.

To further investigate the impaired muscle regeneration in vivo caused by decreased laminin-α2 expression in the TIS7$^{-/-}$ skeletal muscle, we tried supplementation with purified laminins to rescue the differentiation potential of TIS7$^{-/-}$ MSCs. Laminin supplementation partially rescued the fusion defect of TIS7$^{-/-}$ MSCs but not the cytomorphology of the myotubes. These findings suggest that other myogenic factors which are misregulated in TIS7$^{-/-}$ MSCs, such as MyoD and myogenin, are equally important for MSC differentiation. Interestingly, we observed an increase in laminin-α2 expression in TIS7-CT MSCs. This observation raises the possibility that TIS7 directly or indirectly regulates the expression of surface adhesion molecules involved in fusion and differentiation, consistent with its described role as a transcriptional coregulator (22).

Role of TIS7 in adult muscle regeneration in vivo. The results of the experiments described in this study suggest that TIS7 may play a critical role during MSC fusion and differentiation in vivo during adult muscle regeneration. Interestingly, in early phases of adult muscle regeneration, TIS7 protein expression was transiently increased and localized to the central myonuclei of the regenerating muscle fibers in the TIS7$^{+/+}$ soleus muscle. Following MCD, cytoplasmic factors are released from muscle tissue to stimulate the proliferation of the quiescent organotypic stem cells, the MSCs. These proliferating MSCs, largely residing within the common basal lamina, usually fuse to form myotubes and finally a normal muscle fiber (11). Additionally, the possibility that SKMc15, the TIS7 homologue (present in the earliest stages of development [days

TIS7$^{-/-}$ to unlabeled TIS7$^{+/+}$ cells (4ϕ:1) (b), labeled TIS7$^{-/-}$ to unlabeled TIS7$^{+/+}$ cells (1ϕ:4) (c), and labeled TIS7$^{+/+}$ to unlabeled TIS7$^{+/+}$ cells (1ϕ:1) (d). After 5 days of differentiation, cells were fixed and stained with antibody MF20, which is reactive with MHC (green). Note the complete absence of fluorescence-labeled nuclei in myotubes containing more than two nuclei (a, b, and c) and the normal differentiation of TIS7$^{+/+}$ myotubes (d). (e) Determination of fusion indices indicated an increase in the fusion potential of cocultures of TIS7$^{-/-}$ MSCs and TIS7$^{+/+}$ MSCs with an increase in the number of TIS7$^{+/+}$ MSCs. Values below columns correspond to the same labels in panels a to d; error bars indicate standard deviations. Fusion indices were calculated as described in the legend to Fig. 4. Bar, 20 μm.

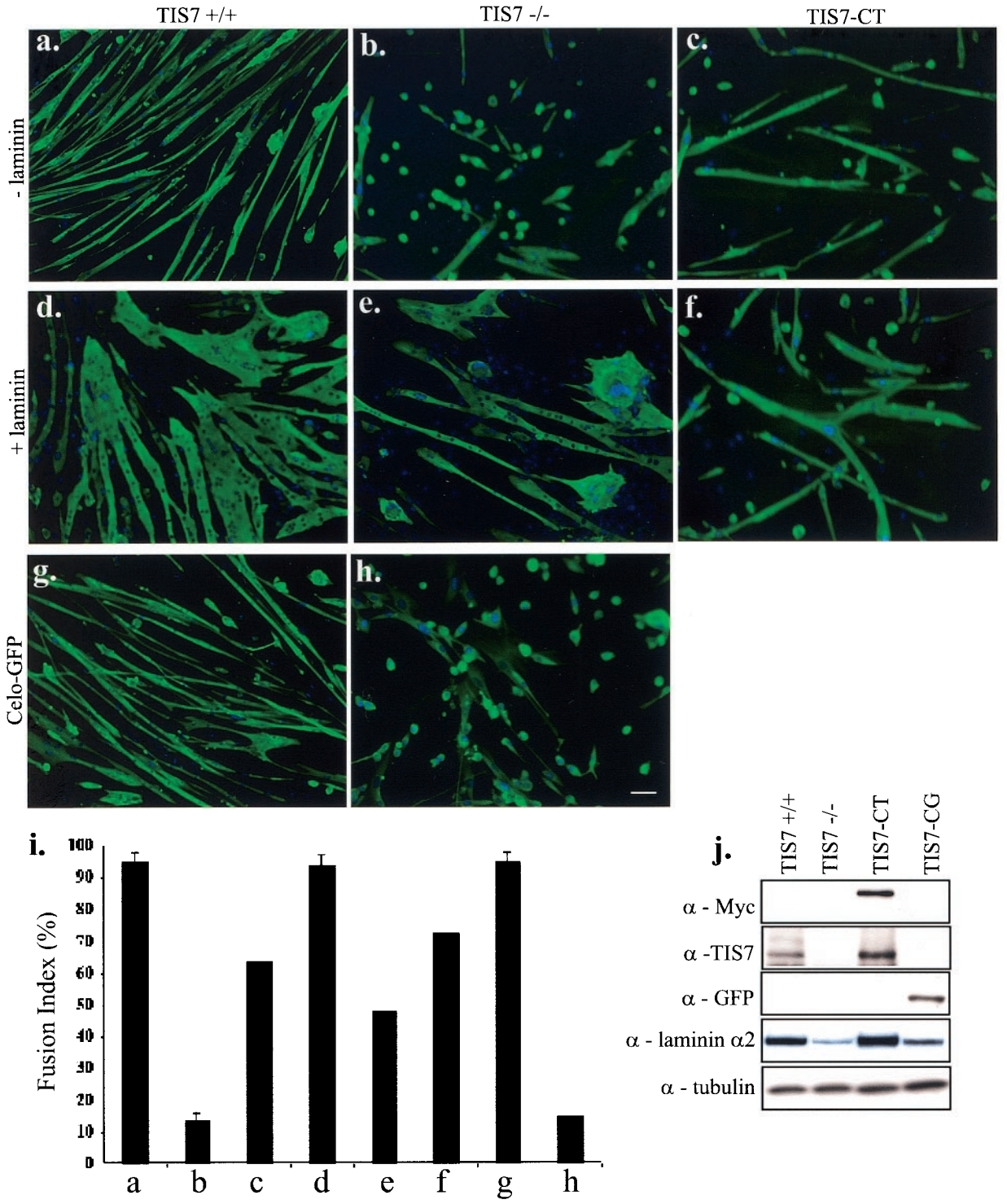

FIG. 6. Rescue of the differentiation deficiency in TIS7$^{-/-}$ MSCs by forced expression of TIS7 or by laminin supplementation. (a) TIS7$^{+/+}$ MSCs fused to form myotubes when exposed to differentiation medium (DM). (b) TIS7$^{-/-}$ MSCs displayed a significant loss of fusion potential when exposed to DM. (c) TIS7$^{-/-}$ MSCs infected with recombinant Celo-TIS7 virus (TIS7-CT cultures) and exposed to DM for 5 days exhibited increased numbers of differentiated myocytes, as detected with antiserum MF20 reactive with MHC, and the formation of elongated bipolar multinucleated myotubes was restored (day 3, MF20). (d) Laminin supplementation enhances the fusion potential of TIS7$^{+/+}$ MSCs. (e) TIS7$^{-/-}$ cells supplemented with laminins exhibited increased numbers of differentiated myotubes, and the formation of multinucleated myotubes was restored. Note the malformed unpolar multinucleated myotubes in TIS7$^{-/-}$ cells supplemented with laminins. (f) The defect in TIS7$^{-/-}$ MSC cytomorphology in DM (supplemented with laminin) could be partially rescued by Celo-TIS7 virus infection. (g) The isotypic Celo-GFP virus control did not affect the fusion potential of TIS7$^{+/+}$ MSCs. (h) The differentiation and fusion potential of TIS7$^{-/-}$ MSCs remained unaltered after infection with an isotypic Celo-GFP virus control. Bar, 20 μm. (i) Fusion indices indicated a fourfold increase in the fusion potential of TIS7-CT cells relative to uninfected TIS7$^{-/-}$ cells. Labels below columns correspond to the same labels in panels a to h; error bars indicate standard deviations. Fusion indices were calculated as described in the legend to Fig. 4. (j) Western blot analysis revealed the expression of TIS7 protein in TIS7$^{+/+}$ MSCs and its absence in TIS7$^{-/-}$ MSCs or TIS7-CG cells. GFP expression was detected with anti-GFP antibody. However, pools of TIS7-CT cells expressed readily detectable TIS7 protein, as detected by the Myc tag in the Celo-TIS7 virus protein.

7.5 to 9]) (3), can rescue TIS7$^{-/-}$ mice from embryonic lethality also cannot be excluded. The human SKMc15 gene was cloned and shown to be a true homologue of the TIS7 gene (13). The significant sequence similarity between TIS7 and SKMc15 proteins could account for the less severe phenotype in TIS7$^{-/-}$ mice during adult muscle regeneration. Our preliminary results indicate that TIS7 and SKMc15 are both present in skeletal muscles, suggesting that the presence of SKMc15 in TIS7$^{-/-}$ mice during muscle regeneration may facilitate MSC differentiation in vivo. The question of whether adult muscle regeneration can occur normally in the absence of TIS7 and SKMc15 should be clarified by the generation of SKMc15 knockout mice and/or TIS7-SKMc15 double-knockout mice.

Our description of an adult skeletal muscle regeneration phenotype in TIS7$^{-/-}$ mice indicates a novel regulatory role for TIS7 in MSC differentiation and fusion during adult muscle regeneration. Future transgenic and mutant crosses may clarify other myogenic factors that are involved in the TIS7$^{-/-}$ myogenic cell differentiation program. Further studies of TIS7$^{-/-}$ mice not only should facilitate molecular analysis of the roles of TIS7 in skeletal muscle but also should allow study of the function of TIS7 in the maintenance and survival of other tissues.

ACKNOWLEDGMENTS

We thank all of the employees of the animal house facility of the Institute of Molecular Pathology and especially E. Wagner and H. C. Theussl for help and advice in generating and maintaining the knockout mice. We thank M. Busslinger, R. Vanishree, and B. Flucher for critically reading and discussing the manuscript. We also thank M. Cotten for the indispensable work in generating recombinant Celo-TIS7 virus. We are grateful to C. Seiser, T. Partridge, and R. Bittner for many helpful discussions and suggestions during the early phases of this project. We thank K. Pfaller, K. Paiha, S. Briel, J. Heckroth, and R. Kofler for excellent technical assistance.

This work was supported by Boehringer Ingelheim, Austrian Science Foundation grant FWF,P13577-GEN, and the Austrian Genome Program (GEM-AU).

REFERENCES

1. **Adams, J. C., and F. M. Watt.** 1993. Regulation of development and differentiation by the extracellular matrix. Development **117:**1183–1198.
2. **Arenander, A. T., J. de Vellis, and H. R. Herschman.** 1989. Induction of c-fos and TIS genes in cultured rat astrocytes by neurotransmitters. J. Neurosci. Res. **24:**107–114.
3. **Buanne, P., B. Incerti, D. Guardavaccaro, V. Avvantaggiato, A. Simeone, and F. Tirone.** 1998. Cloning of the human interferon-related developmental regulator (IFRD1) gene coding for the PC4 protein, a member of a novel family of developmentally regulated genes. Genomics **51:**233–242.
4. **Collins, R. A., and M. D. Grounds.** 2001. The role of tumor necrosis factor-alpha (TNF-alpha) in skeletal muscle regeneration. Studies in TNF-alpha$^{-/-}$ and TNF-alpha$^{-/-}$/LT-alpha$^{-/-}$ mice. J. Histochem. Cytochem. **49:** 989–1001.
5. **Garcia-Alonso, L., R. D. Fetter, and C. S. Goodman.** 1996. Genetic analysis of laminin A in Drosophila: extracellular matrix containing laminin A is required for ocellar axon pathfinding. Development **122:**2611–2621.
6. **Grounds, M. D.** 1999. Muscle regeneration: molecular aspects and therapeutic implications. Curr. Opin. Neurol. **12:**535–543.
7. **Guardavaccaro, D., M. T. Ciotti, B. W. Schafer, A. Montagnoli, and F. Tirone.** 1995. Inhibition of differentiation in myoblasts deprived of the interferon-related protein PC4. Cell Growth Differ. **6:**159–169.
8. **Gumbiner, B. M.** 1996. Cell adhesion: the molecular basis of tissue architecture and morphogenesis. Cell **84:**345–357.
9. **Henchcliffe, C., L. Garcia-Alonso, J. Tang, and C. S. Goodman.** 1993. Genetic analysis of laminin A reveals diverse functions during morphogenesis in Drosophila. Development **118:**325–337.
10. **Huijbregts, J., J. D. White, and M. D. Grounds.** 2001. The absence of MyoD in regenerating skeletal muscle affects the expression pattern of basement membrane, interstitial matrix and integrin molecules that is consistent with delayed myotube formation. Acta Histochem. **103:**379–396.
11. **Irintchev, A., and A. Wernig.** 1987. Muscle damage and repair in voluntarily running mice: strain and muscle differences. Cell Tissue Res. **249:**509–521.
12. **Juliano, R. L., and S. Haskill.** 1993. Signal transduction from the extracellular matrix. J. Cell Biol. **120:**577–585.
13. **Latif, F., F. M. Duh, S. Bader, Y. Sekido, H. Li, L. Geil, B. Zbar, J. D. Minna, and M. I. Lerman.** 1997. The human homolog of the rodent immediate early response genes, PC4 and TIS7, resides in the lung cancer tumor suppressor gene region on chromosome 3p21. Hum. Genet. **99:**334–341.
14. **LeCouter, J. E., P. F. Whyte, and M. A. Rudnicki.** 1996. Cloning and expression of the Rb-related mouse p130 mRNA. Oncogene **12:**1433–1440.
15. **Lentz, S. I., J. H. Miner, J. R. Sanes, and W. D. Snider.** 1997. Distribution of the ten known laminin chains in the pathways and targets of developing sensory axons. J. Comp. Neurol. **378:**547–561.
16. **Megeney, L. A., B. Kablar, K. Garrett, J. E. Anderson, and M. A. Rudnicki.** 1996. MyoD is required for myogenic stem cell function in adult skeletal muscle. Genes Dev. **10:**1173–1183.
17. **Michou, A. I., H. Lehrmann, M. Saltik, and M. Cotten.** 1999. Mutational analysis of the avian adenovirus CELO, which provides a basis for gene delivery vectors. J. Virol. **73:**1399–1410.

17a. **Sabourin, L. A., A. Girgis-Gabardo, P. Seale, A. Asakura, and M. A. Rudnicki.** 1999. Reduced differentiation potential of primary MyoD$^{-/-}$ myogenic cells derived from adult skeletal muscle. J. Cell. Biol. **144:**631–643.

18. **Sastry, S. K., and A. F. Horwitz.** 1996. Adhesion-growth factor interactions during differentiation: an integrated biological response. Dev. Biol. **180:**455–467.
19. **Schwartz, M. A., and D. E. Ingber.** 1994. Integrating with integrins. Mol. Biol. Cell **5:**389–393.
20. **Varnum, B. C., R. W. Lim, and H. R. Herschman.** 1989. Characterization of TIS7, a gene induced in Swiss 3T3 cells by the tumor promoter tetradecanoyl phorbol acetate. Oncogene **4:**1263–1265.
21. **Vietor, I., T. Bader, K. Paiha, and L. A. Huber.** 2001. Perturbation of the tight junction permeability barrier by occludin loop peptides activates beta-catenin/TCF/LEF-mediated transcription. EMBO Rep. **2:**306–312.
22. **Vietor, I., S. K. Vadivelu, N. Wick, R. Hoffman, M. Cotten, C. Seiser, I. Fialka, W. Wunderlich, A. Haase, G. Korinkova, G. Brosch, and L. A. Huber.** 2002. TIS7 interacts with the mammalian SIN3 histone deacetylase complex in epithelial cells. EMBO J. **21:**4621–4631.
23. **Walsh, K., and H. Perlman.** 1997. Cell cycle exit upon myogenic differentiation. Curr. Opin. Genet. Dev. **7:**597–602.
24. **Wernig, A., M. Zweyer, and A. Irintchev.** 2000. Function of skeletal muscle tissue formed after myoblast transplantation into irradiated mouse muscles. J. Physiol. **522:**333–345.
25. **Xu, H., X. R. Wu, U. M. Wewer, and E. Engvall.** 1994. Murine muscular dystrophy caused by a mutation in the laminin alpha 2 (Lama2) gene. Nat. Genet. **8:**297–302.
26. **Yarnitzky, T., and T. Volk.** 1995. Laminin is required for heart, somatic muscles, and gut development in the Drosophila embryo. Dev. Biol. **169:** 609–618.